Mechanisms of transition between $1q$ and $2q$ incommensurate phases in a two-dimensional crystal model

S. V. Dmitriev,* T. Shigenari, and K. Abe
Department of Applied Physics and Chemistry, University of Electro-Communications, Chofu-shi, Tokyo 182, Japan
(Received 23 December 1997; revised manuscript received 17 March 1998)

The two-dimensional elastically hinged molecule model of a crystal which contains two anharmonic terms was studied numerically. The results show that the $1q$ or $2q$ incommensurate phase can be stable depending on the parameters of the model. For example, in the sinusoidal incommensurate regime the $1q$ ($2q$) phase can be globally stable but in the domain-wall regime the situation can be opposite and the $1q \leftrightarrow 2q$ ($2q \leftrightarrow 1q$) transition can be expected. Another mechanism of the $1q \leftrightarrow 2q$ phase transition stems from the softening of the dispersion surface simultaneously at two points of the Brillouin zone, $(\kappa_x,0)$ and $(0,\kappa_y)$. In this case the $2q$ modulated phase can appear as a linear combination of the two $1q$ modulated phases. Under the assumption that the dispersion surface is slightly perturbed for some reason, the softening first occurs at one of the two points resulting in the $1q$ phase formation. Further changing of the external parameters leads to the softening at the second point and the $1q \rightarrow 2q$ transition can take place. Both these mechanisms of the $1q \leftrightarrow 2q$ phase transition were revealed and studied. [S0163-1829(98)07029-5]

I. INTRODUCTION

Recently there has been a growing interest in incommensurate (IC) phases which can appear in a temperature range between two different commensurate phases.[1–3] An IC phase is the modulated phase in which the ratio between lattice period and period of modulation is an irrational number. In many numerical studies, there is no way to determine the exact magnitude of the ratio, therefore, it may be expressed by an irreducible fraction with a big denominator.[4] If the denominator is not big and is not small then the modulated phase is called a high-order commensurate phase.

The IC phase appears from a normal (high-symmetry) commensurate phase as a result of a second-order phase transition and close to the critical point the modulation in a crystal has the form of sinusoidal waves. More often, the modulation can be characterized by a unique wave vector and the IC phase is said to be $1q$ modulated phase, but there are cases where the modulation is described by two or more wave vectors, then it is designated as the $2q$ phase and so on. At lower temperature, as a result of a first-order phase transition (lock-in transition), the IC phase generally gives way to a low-symmetry commensurate phase.

The IC phase can perform different kinds of rather complicated transformations. For example, the pressure-temperature phase diagram of Rb_2ZnBr_4 contains a region where the length of the modulation wave vector of the $1q$ modulated phase exhibits stepwise behavior as a function of pressure.[5]

Not only the length of the modulation wave vector can change. Another example of the IC phase transformation is a transition between $1q$ and $2q$ or $3q$ phases. For example, on cooling in biphenyl, $C_{12}H_{10}$, the sequence of phases is as follows: normal, $2q$, $1q$;[6] in quartz, SiO_2, as follows: normal, $1q$, $3q$, commensurate;[7,8] in barium sodium niobate, $Ba_2NaNb_5O_{15}$, as follows: normal, $2q$, $1q$, commensurate;[9,10] and in $Cu_{0.78}Pd_{0.22}$ alloy as follows: high-symmetry disordered (normal), $2q$, $1q$.[11]

The kinetics of the $2q \rightarrow 1q$ phase transition in the $Cu_{0.78}Pd_{0.22}$ alloy has been studied by Bohr, Broddin, and Loiseau[11] by time-resolved x-ray scattering.

There are several kinds of microscopic models which support the modulated structure.

In the frame of the axial next-nearest-neighbor Ising (ANNNI) model the variable assigned to each particle can obtain discrete values from a given set. It is very natural in some applications, for example, in the physics of ordered alloys where this variable means the sort of atom in a lattice point. The physical mechanism responsible for the formation of modulated structures is the competing interactions.[12,13] The influence of the temperature and the features of the domain walls have been studied in the frame of the mean-field approach when the set of the possible states of a particle is no longer discrete.[14,15] At finite temperatures the ANNNI model has a very rich phase diagram with different modulated commensurate and IC phases.[13,14] The similar behavior shows the model with the spin anisotropy for which the spins vary continuously.[16] Phase diagrams obtained using the mean-field approximation appear to be correct in all but minor details.[12] The ANNNI model modified by Yamada and Hamaya[17] qualitatively describe the chain of transformations containing IC high-order commensurate, and commensurate phases for various dielectrics of A_2BX_4 family.

For the description of the IC phase in dielectrics, however, the spin variable seems not as natural as in the case of ordered alloys. Here the displacement of the particle is usually taken as a natural variable.[4,18–27] The elastically hinged molecule (EHM) model studied in this paper belongs to this second class of microscopic models.

The $3q \rightarrow 3q'$ phase transition, with a change of the modulation wavelength, has been simulated by Parlinski and Chapuis[18] by a molecular-dynamics technique in the frame of the three-dimensional hexagonal model. The molecular-dynamics investigation of the kinetics of the $1q \rightarrow 3q$ and $3q \rightarrow 1q$ phase transitions in the three-dimensional hexago-

nal model has been performed by Parlinski and Chapuis.[18,21] It has been found that the $1q \rightarrow 3q$ transition originates from the nucleation of a set of antistripples within the stripes of the $1q$ phase.[18] In the $3q \rightarrow 1q$ transition the columns (cells of the $3q$ phase) merge together and form a stripe of the $1q$ phase.[18,21]

It has been shown by Parlinski *et al.* that to obtain the stable $2q$ and $3q$ IC phases, special anharmonic terms should be introduced into the Hamiltonian.[18,21–23] After these works the conditions of the existence of the stable $2q$ and $3q$ IC phases in two- and three-dimensional microscopic models are quite clear, however the $1q \leftrightarrow 2q$ and $1q \leftrightarrow 3q$ phase transitions have not been adequately investigated.

In this paper the one-dimensional elastically hinged molecule (EHM) model recently proposed by the present authors[24,25] was extended to the two-dimensional EHM model. The Hamiltonian of the last model is similar to that studied by Parlinski,[22] with two distinctions.

First, the harmonic part of the two-dimensional EHM model describes a crystal with any anisotropy and subjected to arbitrary homogeneous deformation, whereas the Parlinski's model considers a crystal with a particular case of anisotropy and subjected to a hydrostatic pressure. As a result, in the two-dimensional EHM model the softening of a mode with any wave vector is possible, whereas in the Parlinski's model the softening can occur at a point (κ,κ) or simultaneously at two points $(\kappa,0)$ and $(0,\kappa)$ or simultaneously at an infinitely large number of points of the Brillouin zone. One will see that the mechanism of the $1q \leftrightarrow 2q$ phase transition discussed in Sec. IV B cannot be studied in the frame of the model of Parlinski.

The second distinction is that the anharmonic part of the Hamiltonian of the EHM model contains a four-body term describing the interaction of each hinge with the nearest and next-nearest neighbors instead of the three-body term describing the interaction of each hinge with the nearest neighbors, as it is in the Parlinski's model. The necessity of this revision for our calculations will be explained in Sec. IV A.

This paper is organized as follows: In Sec. II the two-dimensional EHM model is introduced. In Sec. III the conditions of softening of the dispersion surface are given. In Sec. IV the two mechanisms of the $1q \leftrightarrow 2q$ phase transition are discussed and illustrated by numerical examples and Sec. V concludes the paper.

II. TWO-DIMENSIONAL EHM MODEL

The one-dimensional EHM model of a crystal is a chain of molecules which are connected with each other by the elastic hinges. Each hinge of the one-dimensional EHM model has one degree of freedom, namely, the transversal displacement u_j. The chain is compressed by the force along its axis and the hinges are in the anharmonic, one-well fourth-order polynomial background potential. In dimensionless form the equations of motion are[24]

$$\frac{d^2u_j}{dt^2} + F(u_{j-2} - 4u_{j-1} + 6u_j - 4u_{j+1} + u_{j+2}) + P(u_{j-1} - 2u_j + u_{j+1}) + u_j + u_j^3 = 0, \tag{2.1}$$

where coefficients $F>0$, $P>0$ are proportional to the stiffness of a hinge and the compression force, respectively. Note that the model with different physical interpretation but governed by essentially the same equation of motion has been studied earlier by Slot and Janssen[26] and by Ishibashi.[27]

In the continuum limit Eq. (2.1) takes the form

$$\frac{\partial^2 u}{\partial t^2} + F\frac{\partial^4 u}{\partial x^4} + P\frac{\partial^2 u}{\partial x^2} + u + u^3 = 0, \tag{2.2}$$

where the displacement $u(x,t)$ is the unknown function, coefficients F and P describe the elastic properties of media and the external pressure, respectively. An obvious two-dimensional generalization of Eq. (2.2) is

$$\frac{\partial^2 u}{\partial t^2} + F_x\frac{\partial^4 u}{\partial x^4} + 2F_{xy}\frac{\partial^4 u}{\partial x^2 \partial y^2} + F_y\frac{\partial^4 u}{\partial y^4} + P_x\frac{\partial^2 u}{\partial x^2} + P_y\frac{\partial^2 u}{\partial y^2} + u + u^3 = 0, \tag{2.3}$$

where $u(x,y,t)$ is the unknown function, F_x, F_{xy}, F_y are the elastic constants of the anisotropic media and P_x, P_y are the components of the external pressure. Equation (2.3) has long been in use in the theory of plates.[28]

The discrete analog of Eq. (2.3) is

$$\frac{d^2u_{j,l}}{dt^2} + (1 - 2P_x - 2P_y + 6F_x + 8F_{xy} + 6F_y)u_{j,l} + u_{j,l}^3 + F_x(u_{j-2,l} + u_{j+2,l}) + F_y(u_{j,l-2} + u_{j,l+2}) + 2F_{xy}(u_{j+1,l+1} + u_{j-1,l+1} + u_{j+1,l-1} + u_{j-1,l-1}) + (P_x - 4F_x - 4F_{xy})(u_{j-1,l} + u_{j+1,l}) + (P_y - 4F_y - 4F_{xy})(u_{j,l-1} + u_{j,l+1}) + S(u_{j-1,l-1}u_{j+1,l}u_{j,l+1} + u_{j+1,l-1}u_{j,l+1}u_{j-1,l} + u_{j+1,l+1}u_{j-1,l}u_{j,l-1} + u_{j-1,l+1}u_{j,l-1}u_{j+1,l}) = 0, \tag{2.4}$$

where we have introduced an additional anharmonic term with coefficient S. This fourth-order potential describes the four-body anharmonic interaction of each hinge with the nearest and next-nearest neighbors.

Equation (2.4) is the equation for motion of the (j,l)th hinge of the two-dimensional EHM model. The Hamiltonian of the two-dimensional EHM model is

$$H=\frac{1}{2}\sum_{j,l}\left(\frac{du_{j,l}}{dt}\right)^2+\frac{1}{2}(1-2P_x-2P_y+6F_x+8F_{xy}+6F_y)\sum_{j,l}u_{j,l}^2+\frac{1}{4}\sum_{j,l}u_{j,l}^4+\frac{1}{2}\sum_{j,l}u_{j,l}[F_x(u_{j-2,l}+u_{j+2,l})$$
$$+F_y(u_{j,l-2}+u_{j,l+2})]+F_{xy}\sum_{j,l}u_{j,l}(u_{j+1,l+1}+u_{j-1,l+1}+u_{j+1,l-1}+u_{j-1,l-1})+\frac{1}{2}(P_x-4F_x-4F_{xy})$$
$$\times\sum_{j,l}u_{j,l}(u_{j-1,l}+u_{j+1,l})+\frac{1}{2}(P_y-4F_y-4F_{xy})\sum_{j,l}u_{j,l}(u_{j,l-1}+u_{j,l+1})+\frac{S}{4}\sum_{j,l}u_{j,l}(u_{j-1,l-1}u_{j+1,l}u_{j,l+1}$$
$$+u_{j+1,l-1}u_{j,l+1}u_{j-1,l}+u_{j+1,l+1}u_{j-1,l}u_{j,l-1}+u_{j-1,l+1}u_{j,l-1}u_{j+1,l}). \tag{2.5}$$

Several physical interpretations of the Hamiltonian Eq. (2.5) are possible. The first one, used by Parlinski,[22] considers the square lattice of the interacting pointwise particles. The EHM model gives another interpretation.[24] Recall that many dielectric crystals are built of the clusters of atoms which can be considered as almost undeformable, e.g., quartz consists of the almost rigid SiO_4 tetrahedral clusters joined to each other, and the oxygen atoms at vertices play the role of hinges. Keeping this in mind, one can consider a two-dimensional layer of rigid molecules joined to each other by the elastic hinges (see Fig. 1). If the angle between the axes of the neighboring molecules is not equal to 0, the elastic hinge produces the moments which tend to decrease the absolute value of the angle. The stiffness of the anisotropic hinge is characterized by the coefficients F_x, F_y, F_{xy}. Each hinge has one degree of freedom which is a displacement perpendicular to the xy plane. (In the quartz case, it corresponds to the rotation angle of SiO_4 tetrahedra.) The hinges are in the anharmonic background potential $(1/2)u_{j,l}^2+(1/4)u_{j,l}^4$ which describes the influence of the rest of the crystal on the considered layer of molecules. The crystal is subjected to the external pressure P_x, P_y.

The Hamiltonian similar to Eq. (2.5) can be obtained also as a mean-field approximation to an ANNNI model. For example, the harmonic part of the Hamiltonian of the one-dimensional EHM model[24] is essentially the same as that for the mean-field Hamiltonian.[12]

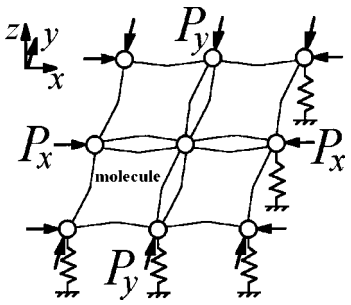

FIG. 1. The two-dimensional EHM model. Rigid molecules are joined to each other by the elastic hinges (open circles). If the angle between the axes of the neighboring molecules is not equal to 0, the elastic hinge produces the moments which tend to decrease the absolute value of the angle. The stiffness of the anisotropic hinge is characterized by the coefficients F_x, F_y, F_{xy}. Each hinge has one degree of freedom which is displacement along z axis. The hinges are in the anharmonic background potential (shown by springs) which describes the influence of the rest of the crystal on the considered layer of molecules. The crystal is subjected to the external pressure P_x, P_y.

III. DISPERSION RELATION

Substituting the formula

$$u_{j,l}=\exp[2\pi i(\kappa_x j+\kappa_y l)-i\omega t] \tag{3.1}$$

into the harmonic part of Eq. (2.4) one obtains the dispersion relation

$$\omega^2(\kappa_x,\kappa_y)=4F_xA^2+8F_{xy}AB+4F_yB^2+2(P_x-4F_x-4F_{xy})A+2(P_y-4F_y-4F_{xy})B+1-2P_x-2P_y+4F_x+8F_{xy}+4F_y, \tag{3.2}$$

where $A=\cos(2\pi\kappa_x)$, $B=\cos(2\pi\kappa_y)$. In Fig. 2 the reciprocal space of the model is shown, where we symbolize the particular points of the Brillouin zone.

In the subsequent discussion the elastic constants F_x, F_{xy}, F_y and the parameter S will be considered temperature dependent. Changing of the temperature and/or changing of the external pressure P_x, P_y leads to the motion of a representative point in the six-dimensional phase space.

Obviously, Eq. (2.4) has the trivial solution $u_{j,l}=0$ (normal phase). This solution is stable when the function $\omega^2(\kappa_x,\kappa_y)$, given by Eq. (3.2), has no negative values. When the representative point moves in the phase space the function Eq. (3.2) changes and it can vanish, i.e., the mode softens, at a certain point (κ_x,κ_y). The vanishing leads to the condensation of the mode

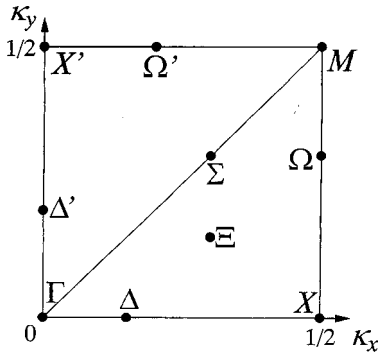

FIG. 2. The reciprocal space of the model. The wave vectors of the modulation waves are denoted by the symbols given in the figure.

$$u_{j,l}=Q_1\cos[2\pi(j\kappa_x+l\kappa_y)+\varphi_1] + Q_2\cos[2\pi(j\kappa_x-l\kappa_y)+\varphi_2], \tag{3.3}$$

where at least one of the coefficients Q_1, Q_2 is not equal to 0. One can see that $\omega^2(0,0)=1$. It means that at least one of the components of the soft mode wave vector (κ_x,κ_y) is not equal to 0 and that the EHM model has no acoustic mode.

As is clear from Eq. (3.2), from $\omega^2(\kappa_x,\kappa_y)=0$ it follows that $\omega^2(\pm\kappa_x,\pm\kappa_y)=0$ with any combination of signs $+$ and $-$. In the following, instead of referring to all the softening points $(\pm\kappa_x,\pm\kappa_y)$, only one of them with $\kappa_x\geqslant 0$, $\kappa_y\geqslant 0$ will be referred to.

Just after the softening the displacements $u_{j,l}$ are small and for this reason Eq. (3.3), which was obtained from the harmonic part of Eq. (2.4), gives a good approximation to a solution of the nonlinear Eq. (2.4). The only problem is to choose the magnitudes of parameters Q_1, Q_2, φ_1, φ_2 in Eq. (3.3) which minimizes the energy of the solution.

If either $\kappa_x=0$ or $\kappa_y=0$ then Eq. (3.3) gives a $1q$ modulated phase. If both κ_x and κ_y are not equal to 0 then the modulated phase may be of the $1q$ or $2q$ type depending on the coefficients Q_1 and Q_2. If the structure Eq. (3.3) has the lowest energy when both Q_1 and Q_2 are not equal to 0 then it corresponds to a $2q$ modulated phase, otherwise to a $1q$ phase.

At some special conditions the softening can occur simultaneously at a few or even at an infinitely large number of points of the Brillouin zone. In such a situation, the displacements of the hinges in modulated phase can be expressed as a linear combination of all the soft modes given by Eq. (3.3).

Let us turn to the description of the conditions of softening of the dispersion surface $\omega^2(\kappa_x,\kappa_y)$. Three different cases should be considered. The first case is the softening at the points M, X, X'. The second case is the softening at a point Ω, Ω', Δ, or Δ'. The third case is the softening at a general point of the Brillouin zone Ξ. Each case will be considered separately.

Case 1. Softening at the point M occurs when

$$1-4P_x-4P_y+16F_x+32F_{xy}+16F_y=0. \tag{3.4}$$

Softening at the point X occurs when

$$1-4P_x+16F_x=0, \tag{3.5}$$

and at the point X' when

$$1-4P_y+16F_y=0. \tag{3.6}$$

Case 2. The dispersion surface vanishes at a point Ω when $\omega^2(1/2,\kappa_y)=0$ and $\partial\omega^2/\partial\kappa_y=0$. These conditions give

$$(8F_{xy}-P_y)^2-4F_y(16F_x-4P_x+1)=0. \tag{3.7}$$

Similarly, the softening at a point Ω' takes place when

$$(8F_{xy}-P_x)^2-4F_x(16F_y-4P_y+1)=0. \tag{3.8}$$

The softening takes place at a point Δ' when $\omega^2(0,\kappa_y)=0$, $\partial\omega^2/\partial\kappa_x=0$ and $\partial\omega^2/\partial\kappa_y=0$. It gives

$$P_y^2-4F_y=0. \tag{3.9}$$

In a similar manner one can obtain the condition of softening at a point Δ in the form

$$P_x^2-4F_x=0. \tag{3.10}$$

Case 3. The softening at a general point of the Brillouin zone Ξ occurs when $\omega^2(\kappa_x,\kappa_y)=0$, $\partial\omega^2/\partial\kappa_x=0$, and $\partial\omega^2/\partial\kappa_y=0$. The last two conditions are equivalent to the set of equations

$$\begin{aligned} F_xA+F_{xy}B&=F_x+F_{xy}-P_x/4,\\ F_{xy}A+F_yB&=F_y+F_{xy}-P_y/4. \end{aligned} \tag{3.11}$$

The set of linear equations in A, B Eq. (3.11) has a unique solution

$$A=1+\frac{P_yF_{xy}-P_xF_y}{4(F_xF_y-F_{xy}^2)},\quad B=1+\frac{P_xF_{xy}-P_yF_x}{4(F_xF_y-F_{xy}^2)} \tag{3.12}$$

only if $F_xF_y-F_{xy}^2\neq 0$. In the case of isotropic model ($F_x=F_{xy}=F_y$) this condition is not fulfilled and Eq. (3.11) has no solutions for $P_x\neq P_y$ and has an infinite number of solutions for hydrostatic pressure $P_x=P_y=P$. Physically it means that for the isotropic model the dispersion surface cannot vanish at the considered part of the Brillouin zone when $P_x\neq P_y$ but in a particular case of hydrostatic pressure the softening takes place simultaneously at an infinite number of points.

The condition of softening of the dispersion surface at a general point of the Brillouin zone Ξ may be written as

$$\begin{aligned} &4F_xA^2+8F_{xy}AB+4F_yB^2+2(P_x-4F_x-4F_{xy})A\\ &+2(P_y-4F_y-4F_{xy})B+1-2P_x-2P_y+4F_x\\ &+8F_{xy}+4F_y=0, \end{aligned} \tag{3.13}$$

where A, B are given by Eq. (3.12).

IV. MECHANISMS OF THE $1q\leftrightarrow 2q$ TRANSITION

The modulated phase appears in the EHM model as a result of the second-order phase transition from the normal phase (trivial solution) when at least one of the conditions of softening of the dispersion surface Eqs. (3.4)–(3.10), (3.13) is satisfied.

In the EHM model two scenarios of a $1q\leftrightarrow 2q$ transition can be described. The first possibility is softening of the dispersion surface at a point of the Brillouin zone (κ_x,κ_y) with $\kappa_x\neq 0$ and $\kappa_y\neq 0$. Suppose that just after the softening a $1q$ $(2q)$ modulated phase has lower energy than a $2q$ $(1q)$ phase. Further changing of the external parameters causes the increasing of the influence of the anharmonic terms and the $1q$ $(2q)$ phase may become metastable or even unstable. At this point a transition to the $2q$ $(1q)$ phase can be expected.

Another scenario comes from the possibility of softening of the dispersion surface at two points of the Brillouin zone simultaneously, namely, at a point Δ and at a point Δ'. In this case the $2q$ modulated phase which has the form of a linear combination of the two $1q$ modes may appear. Now suppose that the symmetry of the dispersion surface is bro-

ken for some reason and the softening at the two points occurs not simultaneously. It means that during the changing of the external parameters the softening of the dispersion surface first happens at one of the two points and the $1q$ phase appears. Further changing of the external parameters causes the softening of the dispersion surface at the second point and the $1q \rightarrow 2q$ transition may take place.

The first scenario requires a special type of nonlinearity in the system. In the sinusoidal regime when the influence of the anharmonic terms is small the $1q$ $(2q)$ phase should be globally stable but in the domain-wall regime the unharmonic terms must provide the lowest energy for the $2q$ $(1q)$ phase.

The second scenario requires a special type of the symmetry of the dispersion surface when the softening can occur at two points Δ and Δ' almost simultaneously. Both these mechanisms of the $1q \leftrightarrow 2q$ transition are considered in the following subsections.

A. First mechanism

Discussing the first mechanism the number of parameters of the EHM model can be reduced. Let us restrict ourselves by the case of softening of the dispersion surface at a point of the line $\Sigma(\kappa_x=\kappa_y=\kappa)$. The softening at such a point is possible when $P_x=P_y=P$, $F_x=F_y=F$, and $F_{xy}<F$. To eliminate the parameter F_{xy} let us set $F_{xy}=F/2$. As a result of the assumptions only three parameters P, F, S remain.

The condition of softening at a point Σ Eq. (3.13) in this case reduces to

$$3F-P^2=0, \tag{4.1}$$

which can be used for $F>P/12$. If $F \leqslant P/12$ then the softening occurs at the point M and one must use the condition Eq. (3.4) which takes the form

$$1-8P+48F=0. \tag{4.2}$$

When the representative point moves in the phase space from the region where the trivial solution is stable and crosses the parabola (4.1) at the point with coordinates

$$P(\kappa)=\frac{1}{4}\left[\sin(\pi\kappa)\right]^{-2}, \quad F(\kappa)=\frac{P^2(\kappa)}{3} \tag{4.3}$$

with given

$$\kappa=L/N, \tag{4.4}$$

where $N>2L$ and L, N are coprime positive integers, then the softening of the mode Eq. (3.3) with $\kappa_x=\kappa_y=\kappa$ takes place. If N is rather big then the modulated phase can be considered as an IC phase.

Let us study the case of κ close to 1/4. Substituting the soft mode Eq. (3.3) with $\kappa_x=\kappa_y=1/4$ in the Hamiltonian Eq. (2.5) and minimizing the energy of the soft mode with respect to amplitude and phase Q_1, Q_2, φ_1, φ_2 one can reveal two stable structures. The first stable structure is characterized by

$$Q_1=\sqrt{\frac{2(4P-12F-1)}{1-4S}}, \quad Q_2=0, \quad \varphi_1=\pi/4, \tag{4.5}$$

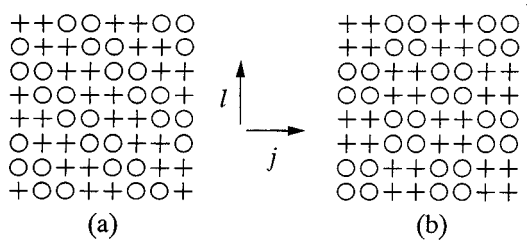

FIG. 3. Displacements of the hinges for (a) $1q$ and (b) $2q$ commensurate phases with $(\kappa_x,\kappa_y)=(1/4,1/4)$ defined by Eqs. (4.6) and (4.9), respectively. Four periodic cells are shown. Hinges with negative and positive displacements are marked by ○ and +, respectively.

which give the solution to Eq. (2.4) in the form of a $1q$ modulated structure

$$u_{j,l}^{1q,1/4}=Q_1\cos\left[\frac{\pi}{2}\left(j+l+\frac{1}{2}\right)\right]. \tag{4.6}$$

The solution Eq. (4.6) has the averaged energy per hinge

$$E^{1q,1/4}=-\frac{(4P-12F-1)^2}{4(1-4S)}. \tag{4.7}$$

The second stable structure is characterized by

$$Q_1=Q_2=\sqrt{\frac{4P-12F-1}{1+4S}}, \quad \varphi_1=\pi/2, \quad \varphi_2=0, \tag{4.8}$$

which give the solution to Eq. (2.4) in the form of $2q$ modulated structure

$$u_{j,l}^{2q,1/4}=Q_1\cos\left[\frac{\pi}{2}\left(j+l+\frac{1}{2}\right)\right]+Q_1\cos\left[\frac{\pi}{2}(j-l)\right]. \tag{4.9}$$

The solution Eq. (4.9) has the averaged energy per a hinge

$$E^{2q,1/4}=-\frac{(4P-12F-1)^2}{4(1+4S)}. \tag{4.10}$$

The phases Eqs. (4.6) and (4.9) cannot be considered as IC phases because for $\kappa=1/4$ one has $N=4$ which is rather small. These phases are the low-symmetry commensurate phases. The displacements in the $1q$ and $2q$ commensurate phases Eqs. (4.6) and (4.9) are shown in Figs. 3(a) and 3(b), respectively, where the hinges with negative and positive displacements are marked by ○ and +, respectively.

From Eqs. (4.7) and (4.10) one can see that if $S=0$ (no anharmonicity), then the $1q$ and $2q$ commensurate phases have the same energy. Let us choose the magnitude $S=-0.2$ at which the energy of the $2q$ phase is lower than the energy of the $1q$ phase. The dimensionality of the phase space was reduced to two.

The anharmonic part of the Hamiltonian which has been used by Parlinski[22] gives no difference between the energies of the solutions Eqs. (4.6) and (4.9). That is why an anharmonic term different from that of Parlinski's model was chosen for the present investigation.

Let us discuss the IC structure by choosing the particular path of the representative point in the (P,F) phase space as follows:

$$P=\text{const}=P(\kappa) \quad \text{with} \quad \kappa=\frac{10}{41}, \tag{4.11}$$

where $P(\kappa)$ is given by Eq. (4.3). The parameter P is fixed and thus the phase space becomes one dimensional.

According to Eq. (4.3), while the representative point moves in the range $F>F(10/41)$, the trivial solution (normal phase) is stable. The point $F(10/41)=F_i$, which can be found from Eq. (4.3), is the point of the phase transition from the normal to the modulated phase. At F_i the softening of the mode (κ,κ) with $\kappa=10/41$ takes place. This mode $(N=41)$ can be considered as an IC phase where the wave vector is close to the wave vector of the low-symmetry commensurate phase $(\kappa=1/4)$. Just after the softening of the mode, in other words, in the vicinity of the F_i the IC phase can be described with high accuracy by the trigonometric functions. The modulated phase may be of the $1q$ type

$$u_{j,l}^{1q,10/41}=Q\ \cos\left[2\pi\ \frac{10}{41}\ (j+l)\right] \tag{4.12}$$

or of the $2q$ type

$$u_{j,l}^{2q,10/41}=Q\ \cos\left[2\pi\ \frac{10}{41}\ (j+l)\right]+Q\ \cos\left[2\pi\ \frac{10}{41}\ (j-l)\right]. \tag{4.13}$$

The amplitude Q in Eqs. (4.12), (4.13) cannot be derived analytically and below it was obtained numerically from the minimum energy condition.

Further motion of the representative point in the phase space (decreasing of F) leads to the increasing of the influence of the anharmonic terms and the sinusoidal regime is changed to the domain-wall regime. In this regime the crystal structure cannot be obtained by minimizing the energy with respect to the only one parameter Q. In order to carry out the minimization of crystal energy with respect to all the displacements $u_{j,l}$ the dissipative term $\delta(du_{j,l})/(dt)$ was introduced in Eq. (2.4), where δ is the viscosity coefficient. Using either Eq. (4.12) or (4.13) as the initial condition and solving numerically the equations of motion Eq. (2.4) with the dissipative term, at the completion of the relaxation one obtains the equilibrium either $1q$ or $2q$ IC phase. The size of the crystallite subjected to the periodic boundary conditions was $N\times N=41\times 41$ hinges which is one period of the IC phase.

In Fig. 4(a) the energy of the $2q$ equilibrium IC phase obtained from the structure Eq. (4.13) by the energy minimization with respect to all the displacements $u_{j,l}$ (solid line) is compared with that obtained by the energy minimization with respect to only one parameter Q (dashed line). The curves coincide in the vicinity of F_i, where the influence of the anharmonic terms is small.

In Fig. 4(b) the energies of the $1q$ and $2q$ equilibrium IC phases with $\kappa=10/41$ are schematically shown by solid and dashed lines, respectively, as the functions of parameter F. One can see that while $F>F_i$ the only equilibrium solution is the trivial solution with zero energy. For $F<F_i$ there is a

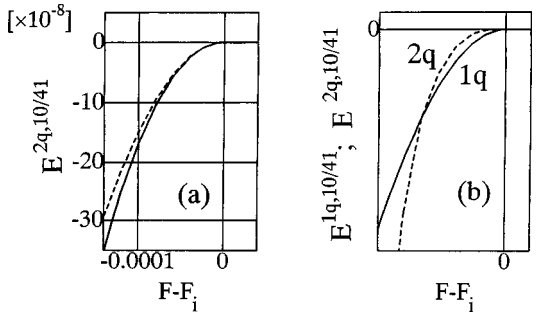

FIG. 4. (a) The F dependence of the energy of the $2q$ equilibrium IC phase obtained from the structure Eq. (4.13) by the energy minimization with respect to all the displacements $u_{j,l}$ (solid line) and with respect to the only one parameter Q (dashed line). (b) Schematic representation of the energies of the $1q$ (solid line) and $2q$ (dashed line) equilibrium IC phases with $\kappa=10/41$ as the functions of parameter F. The $1q$ and $2q$ IC phases were obtained by the relaxation of the structures Eqs. (4.12) and (4.13), respectively. The $1q$ and $2q$ IC phases appear at $F=F_i$. In the range $F<F_i$ first the $1q$ IC phase has lower energy but then the $2q$ phase has lower energy.

range where the energy of the $1q$ structure is lower and this range is followed by the range where the $2q$ structure has lower energy. At the boundary of these two ranges the $1q\leftrightarrow 2q$ transition can be expected.

Let us study the kinetics of the $1q\rightarrow 2q$ transformation. The numerical experiment was performed as follows. The relaxation of the $1q$ IC phase given by Eq. (4.12) was carried out at a magnitude of parameter F from the region where the $2q$ IC phase would have lower energy. As a result of the relaxation the $1q$ phase was obtained. Then the small random perturbation of the hinge displacements was introduced and the relaxation of the system was continued. It was observed that the system does not relax back to the $1q$ equilibrium state for it was unstable but it relaxed to the globally stable $2q$ IC phase.

The kinetics of the $1q\rightarrow 2q$ transformation at $F=F_i-5\times 10^{-4}$ is presented in Fig. 5. The displacements range from $-u_{\max}$ to $u_{\max}$, where $u_{\max}$ is the maximum absolute value of $u_{j,l}$, was divided into five equal parts and the displacement of a hinge is marked in Fig. 5 by one of the signs ○, ◦, ●, +, + depending on the part in which the displacement of the hinge falls. In Fig. 5(a) the $1q$ unstable, slightly perturbed IC phase is presented. The random perturbation of displacements does not exceed $0.001v_{\max}$. In Figs. 5(b) and 5(c), the intermediate stages of the $1q\rightarrow 2q$ transformation are shown. In Fig. 5(d) the globally stable $2q$ IC phase is shown as the final result of the relaxation.

The $1q\rightarrow 2q$ transformation can be discussed in terms of the motion of the domain walls. The domain walls in Fig. 5 appear as the dark strips. In Fig. 5(a), for example, the dark strips separate the domains of the $1q$ commensurate phase shown in Fig. 3(a) whereas in Fig. 5(d) the dark strips separate the domains of the $2q$ commensurate phase shown in Fig. 3(b). The transformation starts from the splitting of the domain wall into two domain walls moving in the opposite directions [compare Figs. 5(a) and 5(b)]. The splitting of the unstable domain walls has been described in the frame of the one-dimensional EHM model.[25] During the phase transition

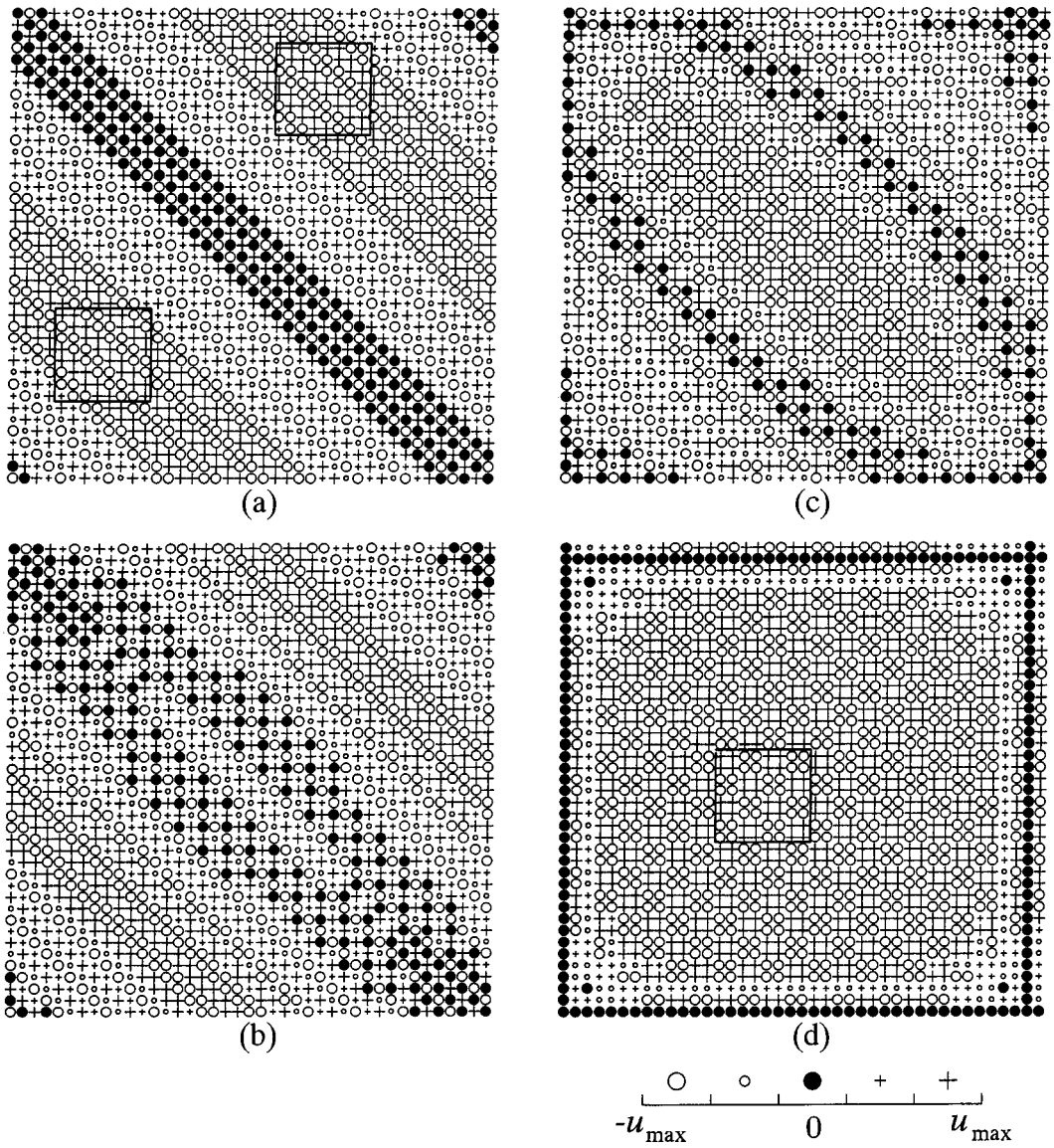

FIG. 5. The kinetics of the $1q \rightarrow 2q$ transition at $F = F_i - 5 \times 10^{-4}$: (a) the $1q$ unstable, slightly perturbed IC phase, (b,c) the intermediate stages of the process, (d) the globally stable $2q$ IC phase. Domain walls appear as dark strips. Inside the squares in (a) there is a $1q$ commensurate phase shown in Fig. 2(a) and inside the square in (d) there is a $2q$ commensurate phase shown in Fig. 2(b).

the set of parallel equidistant domain walls [see Fig. 5(a)] transforms into the rectangular net of domain walls [see Fig. 5(d)].

The results presented in Fig. 5 were obtained on one period of the IC phase. Actually, the picture of the $1q \rightarrow 2q$ transformation may be more complicated due to the random nucleation process of the domain-wall splitting. The net of domain walls in the $2q$ IC phase may be not so fine and rectangular as it is shown in Fig. 5(d).

B. Second mechanism

It is evident from Eqs. (3.9) and (3.10) that the softening simultaneously at the two points $(\kappa_x, 0)$ and $(0, \kappa_y)$ takes place if $P_x^2 - 4F_x = P_y^2 - 4F_y$. Let us consider the particular case of softening at the points $(\kappa,0)$ and $(0,\kappa)$ which takes place in the EHM model with hydrostatic pressure

$$P_x = P_y = P, \tag{4.14}$$

and the anisotropy of a special type

$$F_{xy} > F_x = F_y = F. \tag{4.15}$$

To eliminate the parameter F_{xy} let us set $F_{xy} = 2F$.

In view of Eqs. (4.14), (4.15), both conditions of softening Eqs. (3.9), (3.10) take the form

$$P^2 - 4F = 0, \tag{4.16}$$

which can be used for $F > P/8$. If $F \leqslant P/8$ then the softening occurs at the points X, X' and one must use the conditions Eqs. (3.5), (3.6) which give

$$1 - 4P + 16F = 0. \tag{4.17}$$

When the representative point moves in the phase space from the region where the trivial solution is stable and crosses the parabola (4.16) at the point with coordinates

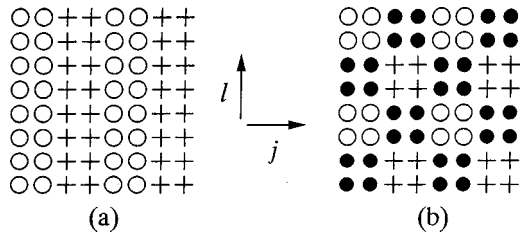

FIG. 6. Displacements of the hinges for (a) $1q$ commensurate phase with $(\kappa_x,\kappa_y)=(1/4,0)$, Eq. (4.19), and (b) $2q$ commensurate phase with two soft modes $(\kappa_x,\kappa_y)=(1/4,0)$ and $(\kappa_x,\kappa_y)=(0,1/4)$, Eq. (4.22). Four periodic cells are shown. Hinges with negative, zero, and positive displacements are marked by the signs ○, ●, and +, respectively.

$$P(\kappa)=\frac{1}{2}\,[\sin(\pi\kappa)]^{-2},\quad F(\kappa)=\frac{P^2(\kappa)}{4},\qquad (4.18)$$

then the softening of the two modes can take place at $(\kappa,0)$ and $(0,\kappa)$, where $\kappa=L/N$, $N>2L$ and L, N are coprime positive integers.

In the following, the case of κ close to 1/4 will be considered. There are two possible stable commensurate structures with $\kappa=1/4$. One is of the $1q$ type

$$u_{j,l}^{1q,1/4}=Q_1\cos\left[\frac{\pi}{2}\left(j+\frac{1}{2}\right)\right] \qquad (4.19)$$

with

$$Q_1=\sqrt{\frac{2(2P-4F-1)}{1-4S}} \qquad (4.20)$$

and averaged energy per hinge

$$E^{1q,1/4}=-\frac{(2P-4F-1)^2}{4(1-4S)}. \qquad (4.21)$$

Another one is of the $2q$ type

$$u_{j,l}^{2q,1/4}=Q_1\cos\left[\frac{\pi}{2}\left(j+\frac{1}{2}\right)\right]+Q_1\cos\left[\frac{\pi}{2}\left(l+\frac{1}{2}\right)\right] \qquad (4.22)$$

with

$$Q_1=\sqrt{\frac{2P-4F-1}{2(1-S)}} \qquad (4.23)$$

and averaged energy per hinge

$$E^{2q,1/4}=-\frac{(2P-4F-1)^2}{8(1-S)}. \qquad (4.24)$$

The $1q$ and $2q$ low-symmetry commensurate phases given by Eqs. (4.19) and (4.22) are shown in Figs. 6(a) and 6(b), respectively. In Fig. 6 the hinges with negative, zero, and positive displacements are marked by signs ○, ● and +, respectively.

If $S=0$ then the energy of the $2q$ commensurate phase Eq. (4.24) is twice higher than that of the $1q$ commensurate phase Eq. (4.21). Let us set $S=-1$ so that the $2q$ commensurate phase obtains the energy lower than that for the $1q$ commensurate phase.

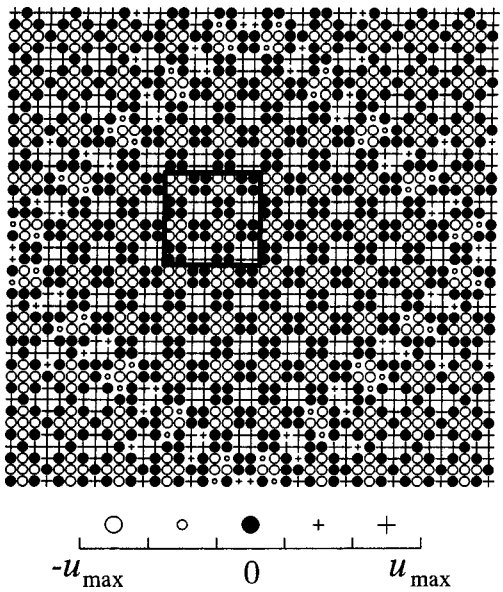

FIG. 7. The $2q$ IC phase obtained as a result of relaxation of the structure Eq. (4.25) at $F=F_i-10^{-3}$, $P_x=P_y=P(10/41)$. Structure inside the square is the $2q$ commensurate phase shown in Fig. 5(b).

To obtain an IC phase let us consider the path of the representative point given by Eq. (4.11) but $P(\kappa)$ must be calculated here from Eq. (4.18). While $F>F_i$, where $F_i=F(10/41)$ can be calculated from Eq. (4.18), the only trivial solution (normal phase) is stable. At F_i the phase transition to the IC phase takes place due to the softening at the two points (10/41, 0) and (0, 10/41). The numerical calculations showed that in the case under consideration the range of stability of the $1q$-IC phase is absent in contrast with the case studied in the previous subsection. The IC phase appeared as the $2q$ modulated phase which in the vicinity of the softening point can be presented as

$$u_{j,l}^{2q,10/41}=Q\,\cos\left(2\pi\,\frac{10}{41}\,j\right)+Q\,\cos\left(2\pi\,\frac{10}{41}\,l\right). \qquad (4.25)$$

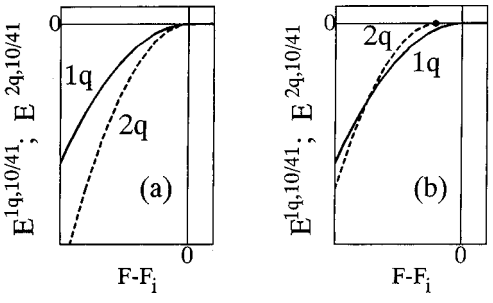

FIG. 8. Schematic representation of the energy of the $1q$ (solid line) and $2q$ (dashed line) equilibrium IC phases for (a) $\varepsilon=0$ and (b) $\varepsilon>0$. The $1q$ and $2q$ IC phases were obtained by the relaxation of the structures Eqs. (4.26) and (4.25), respectively. In (a) the $1q$ and $2q$ IC phases appear at $F=F_i$ and the $2q$ phase has lower energy in the range $F<F_i$. In (b) the $2q$ IC phase appears at F lower than F_i and there is a range where the $1q$ IC phase has lower energy.

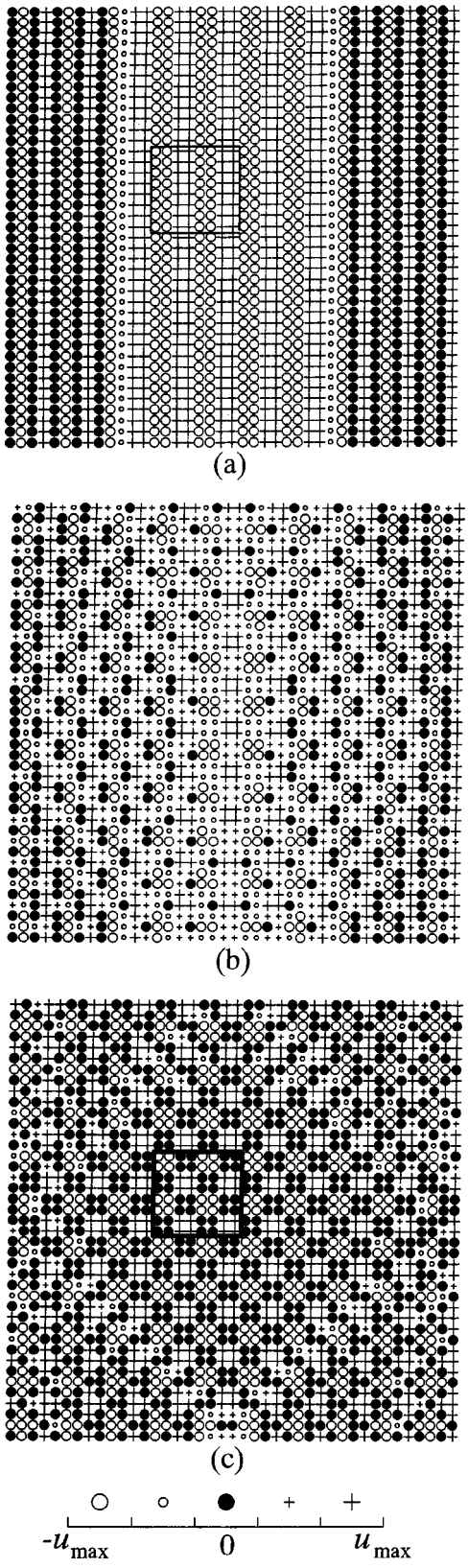

FIG. 9. The kinetics of the $1q \rightarrow 2q$ transition at $F = F_i - 10^{-3}$, $P_x = P(10/41)$, $P_y = P(10/41) - 3 \times 10^{-5}$: (a) the slightly perturbed $1q$ unstable IC phase, (b) an intermediate stage of the process, (c) the globally stable $2q$ IC phase. Structure inside the square in (a) is the $1q$ commensurate phase shown in Fig. 5(a) and inside the square in (c) is the $2q$ commensurate phase, shown in Fig. 5(b).

In Fig. 7 one period of the $2q$ IC phase obtained by the relaxation of the structure Eq. (4.25) at $F = F_i - 10^{-3}$ is shown. The meaning of the signs ○, ∘, ●, +, + is the same as in Fig. 5. As may be seen from Fig. 7, the $2q$ IC phase is the rectangular net of domain walls which separate the domains of the $2q$ commensurate phase shown in Fig. 6(b).

In order to study the $1q \rightarrow 2q$ transition let us suppose that there exists a small deviation from the condition Eq. (4.14), namely, $P_x = P$, $P_y = P - \varepsilon$, where ε is small and, for definiteness, positive. Physically, ε is a small uniaxial stress applied in addition to the hydrostatic pressure P. The presence of such a deviation breaks down the fourfold symmetry of the dispersion surface and softening first occurs at the point (10/41, 0). This softening leads to the $1q$ IC phase formation. In the vicinity of transition point the $1q$ IC phase can be presented as

$$u_{j,l}^{1q,10/41} = Q \cos\left(2\pi \frac{10}{41} j\right). \tag{4.26}$$

Further decreasing of F causes the softening at the point (0, 10/41) and a transition to a $2q$ IC phase happens.

In Fig. 8 the F dependence of the energy of the $1q$ equilibrium IC phase (solid line) is schematically compared to that for the $2q$ equilibrium IC phase (dashed line) at (a) $\varepsilon = 0$ and (b) $\varepsilon > 0$. In (a) the $1q$ and $2q$ IC phases appear at $F = F_i$ and the $2q$ phase has lower energy. In (b) the $2q$ IC phase appears at F lower than F_i and there is a range where the $1q$ IC phase has lower energy.

The kinetics of the $1q \rightarrow 2q$ transformation is shown in Fig. 9 for $\varepsilon = 3 \times 10^{-5}$, $F = F_i - 10^{-3}$. In Fig. 9(a) the slightly perturbed $1q$ unstable IC phase obtained by the relaxation of the structure Eq. (4.26) is presented. The $1q$ IC phase appears as a set of domains of the $1q$ commensurate phase, shown in Fig. 6(a), separated by the vertical domain walls. In Fig. 9(b) an intermediate stage of the structure transformation is shown. In Fig. 9(c) the globally stable $2q$ IC phase is shown as the final result of the relaxation. Structure inside the square in Fig. 9(c) is the $2q$ commensurate phase, shown in Fig. 6(b). Note, that due to the fact that $P_x \neq P_y$ by ε the structure in Fig. 9(c) has no fourfold symmetry and does not coincide with the $2q$ IC phase shown in Fig. 7.

In the example just described the symmetry of the dispersion surface was changed by the violation of the condition Eq. (4.14). Similar results can be also obtained by assuming $F_x = F - \varepsilon$, $F_y = F$ instead of Eq. (4.15).

V. CONCLUSION

The one-dimensional EHM model was generalized to the two-dimensional one. The anharmonic part of the Hamiltonian was chosen in a way to support both $1q$ and $2q$ stable modulated phases. The soft mode can have an arbitrary wave vector (κ_x, κ_y), which has not been shown by the model of Parlinski.[22]

The two mechanisms of the $1q \leftrightarrow 2q$ phase transition were discussed. At the sinusoidal regime of the IC phase the influence of the anharmonic terms is small but it increases in the domain-wall regime. If in the sinusoidal regime the $1q$ $(2q)$ IC phase is globally stable but in the domain-wall re-

gime the $2q$ ($1q$) IC phase becomes globally stable, then the phase transition between them can happen. This is the first mechanism.

In a particular case of the model the dispersion surface has such a symmetry that softening takes place at the two points of the Brillouin zone $(\kappa_x, 0)$, $(0, \kappa_y)$ simultaneously. If this dispersion surface is slightly perturbed by some reason then the softening occurs first at one of the two points with the $1q$ IC phase formation and subsequently at the second point with the possibility of the $1q \rightarrow 2q$ phase transition. This is the second mechanism. The dispersion surface can be perturbed by application of the small uniaxial stress in addition to the hydrostatic pressure P and/or by the anisotropy with a small departure from the condition $F_x = F_y$.

If the phase transition proceeds by the second mechanism then the phase sequence can be only as follows: normal phase $\rightarrow 1q$ phase $\rightarrow 2q$ phase. In the case of the first mechanism the $1q$ and $2q$ phases in this sequence may change places.

ACKNOWLEDGMENTS

The authors are grateful to K. Parlinski for enlightening discussions and suggestions, T. A. Aslanyan for fruitful discussions, and A. A. Vasiliev for the critical reading of the manuscript. S.V.D. wishes to thank the Ministry of Education, Science, Sports, and Culture of Japan for their financial support.

*Permanent address: General Physics Dept., Barnaul State Technical University, 46, Lenin st., 656099, Barnaul, Russia.

[1] *Incommensurate Phases in Dielectrics*, edited by R. Blinc and A. P. Levanyuk (North-Holland, Amsterdam, 1986), Vols. 14.1 and 1.42.
[2] H. Z. Cummins, Phys. Rep. **185**, 211 (1990).
[3] J. C. Tolédano and P. Tolédano, *Landau Theory of Phase Transitions* (World-Scientific, Singapore, 1987).
[4] T. Janssen and J. A. Tjon, Phys. Rev. B **25**, 3767 (1982).
[5] K. Parlinski, R. Currat, C. Vettier, I. P. Aleksandrova, and G. Eckold, Phys. Rev. B **46**, 106 (1992).
[6] See H. Cailleau, in *Incommensurate Phases in Dielectrics* (Ref. 1), Vol. 14.2.
[7] See G. Dolino, in *Incommensurate Phases in Dielectrics* (Ref. 1), Vol. 14.2.
[8] K. Abe, K. Kawasaki, K. Kowada, and T. Shigenari, J. Phys. Soc. Jpn. **60**, 404 (1991).
[9] S. Barré, H. Mutka, C. Roucau, A. Litzler, J. Schneck, J. C. Tolédano, S. Bouffard, and F. Ruller-Albenque, Phys. Rev. B **43**, 11 154 (1991).
[10] See Tolédano, Schneck, and Errandonéa (Ref. 1), Vol. 14.2.
[11] J. Bohr, D. Broddin, and A. Loiseau, Phys. Rev. B **42**, 1052 (1990).
[12] J. M. Yeomans, in *Solid State Physics:* Advances in Research and Applications, edited by H. Ehrenreich and D. Turnbull (Academic, Orlando, 1988), Vol. 41, p. 151.
[13] W. Selke, in *Phase Transitions and Critical Phenomena*, edited by C. Domb and J. L. Lebowitz (Academic, New York, 1992), Vol. 15.
[14] P. Bak and J. von Boehm, Phys. Rev. B **21**, 5297 (1980).
[15] M. E. Fisher and A. M. Szpilka, Phys. Rev. B **36**, 644 (1987).
[16] F. Seno and J. M. Yeomans, Phys. Rev. B **52**, 9550 (1995).
[17] Y. Yamada and N. Hamaya, J. Phys. Soc. Jpn. **52**, 3466 (1983).
[18] K. Parlinski and G. Chapuis, Phys. Rev. B **47**, 13 983 (1993).
[19] R. Currat and T. Janssen, in *Solid State Physics* (Ref. 12), p. 201. Vol. 41.
[20] Z. Y. Chen and M. B. Walker, Phys. Rev. B **43**, 5634 (1991); Phys. Rev. Lett. **65**, 1223 (1990).
[21] K. Parlinski and G. Chapuis, Phys. Rev. B **49**, 11 643 (1994).
[22] K. Parlinski, Phys. Rev. B **48**, 3016 (1993).
[23] K. Parlinski, S. Kwiecinski, and A. Urbanski, Phys. Rev. B **46**, 5110 (1992).
[24] S. V. Dmitriev, K. Abe, and T. Shigenari, J. Phys. Soc. Jpn. **65**, 3938 (1996).
[25] S. V. Dmitriev, T. Shigenari, A. A. Vasiliev, and K. Abe, Phys. Rev. B **55**, 8155 (1997); S. V. Dmitriev, T. Shigenari, and K. Abe, J. Phys. Soc. Jpn. **66**, 2732 (1997); T. Shigenari, A. A. Vasiliev, S. V. Dmitriev, and K. Abe, Ferroelectrics **203**, 335 (1997); S. V. Dmitriev, T. Kumata, T. Shigenari, and K. Abe, J. Korean Phys. Soc. **32**, 907 (1997).
[26] J. J. M. Slot and T. Janssen, Physica D **32**, 27 (1988).
[27] Y. Ishibashi, J. Phys. Soc. Jpn. **60**, 212 (1991).
[28] S. P. Timoshenko and S. Woinowsky-Krieger, *Theory of Plates and Shells* (McGraw-Hill, New York, 1959).